

The "Far Site" Scenario for Gamma-ray Emission in Blazars:

A View from the VLBI Observing Perspective

Iván Agudo^{1,2,3}

¹*Instituto de Astrofísica de Andalucía (CSIC), Apartado 3004, E-18080 Granada, Spain*

²*Institute for Astrophysical Research, Boston University, 725 Commonwealth Avenue, Boston, MA 02215, USA*

³*Current Address: Joint Institute for VLBI in Europe, Postbus 2, NL-7990 AA Dwingeloo, the Netherlands, e-mail: agudo@jive.nl*

Abstract. Since the birth of γ -ray astronomy, locating the origin of γ -ray emission has been a fundamental problem for the knowledge of the emission processes involved. Densely time sampled monitoring programs with very long baseline interferometry and the *Fermi* Gamma-ray Space Telescope, together with several other facilities at most of the available spectral ranges (including polarization measurements if possible) are starting to shed new light for the case of blazars. A successful observing technique consists on analyzing the timing of multi-waveband variations in the flux and linear polarization, as well as changes in ultra-high resolution VLBI images to associate the particularly bright events at different wavebands. Such association can be robustly demonstrated by probing the statistical significance of the correlation among spectral ranges through Monte Carlo simulations. The location of the high energy emission region is inferred through its relative location with regard to the associated low energy event observed in the VLBI images. In this paper, I present some of the latest results using this method that locate the GeV emission within the jets of blazars AO 0235+164 and OJ287 at > 12 pc from the central AGN engine, hence supporting the "far site" scenario.

1 Introduction

Blazars are one of the most exotic classes of active galactic nuclei. This class of active galactic nuclei are characterized by extreme variability of non-thermal radiation from radio to γ -rays. The blazar class is divided into BL Lacertae objects (BL Lacs), and flat spectrum radio quasars (FSRQ, a high power version of the former). The most relevant properties of blazars include superluminal apparent motions up to $40c$ [1], prominent variability of flux and linear polarization on time scales up to minutes, and extreme changes of γ -ray luminosities that are able to exceed those at other energies by up to 3 orders of magnitude. These phenomena are produced in relativistic jets of highly energized, magnetized plasma that are ejected along the rotational poles of the super-massive black-hole/disk system, [e.g. 2], hosted by the active galactic nuclei. Jets in blazars (that point within $\lesssim 10^\circ$ of the line of sight) are affected by prominent relativistic effects that beam their radiation and shorten the variability time scales towards the direction of propagation and give blazars their extreme properties.

Explaining these extreme properties of relativistic jets in blazars remains one of the greatest challenges of high-energy astrophysics. Some of these properties include the location of the γ -ray emitting regions, and the origin of the seed photons responsible for such γ -ray emission. The two competing –although perhaps complementary– scenarios that are currently used to test the problems of the characterization of such properties are the "near site" and the

"far site" scenarios for γ -ray emission in blazars, which are discussed in the following sections.

2 The "Near Site" Scenario

During the latest decades, the "near site" scenario has been the preferred framework to interpret the location of the γ -ray emission site. This scenario is based on the idea that the γ -ray emission region in relativistic jets of blazars is inside the broad line region (BLR), at ~ 0.1 to 1 pc from the central engine of the active galactic nuclei. Since this location is embedded on the dense photon field of the BLR, it has therefore been relatively easy to be treated by most existing one-zone multi-spectral-range emission models to reproduce the γ -ray blazar emission through inverse Compton up-scattering of BLR photons.

The "near site" scenario has been invoked in several works to explain the short time-scales of γ -ray variability of a few hours (or less) reported in some blazars [3–6]. This argument is not being used any more in general. This is because short time scales of variability only imply small emission regions, but not that such regions should be located at any particular location.

A perhaps stronger argument in favor of the γ -ray emission being produced in the "near site" is the one proposed by [7]. These authors explain the sharp breaks at about 5 GeV seen in the γ -ray spectra of some blazars by opacity to pair production by (H and HeII) emission lines in the broad line region. There is anyhow other model that

also needs the γ -ray emission to be located inside the BLR to explain the γ -ray breaks at a few GeV, [e.g. 8]. This alternative model explains the breaks in the γ -ray spectra by the presence of more than one seed photon field in the BLR and their up-scattering to γ -ray energies in the Klein-Nishina regime.

3 The “Far Site” Scenario

The second scenario, on which this paper focuses, is the so called “far site” case. This scenario considers a region much farther away from the central engine (at $\gg 1$ pc, or even a few tens of parsecs from the central engine) where the radiation field from the BLR is not expected to be relevant for inverse Compton scattering up to γ -ray energies. Within the “far site” scenario there are still two main and prominent optical and IR photon fields that need to be considered for their inverse Compton up-scattering. One of them is produced by thermal emission from the dusty torus around the active galactic nuclei, which emits primarily in the IR. The second one is the synchrotron photon field from the jet itself, that radiates prominent emission at all spectral ranges from radio to UV, and even up to X-rays in some cases.

The “far site” scenario has been invoked to explain the positive correlation found between the γ -ray flux and the radio and radio/millimeter flux in large blazar samples as reported by several groups, see [9–17] and Fig. 1. Note that these correlations are not, by themselves, able to locate the site of γ -ray emission in blazars, although they can be easily explained if the γ -ray and the millimeter emission regions are co-spatial, and therefore they are produced far from the photon field of the BLR (as required if the radio and millimeter emission is considered at several to tens of pc from the central black hole of the active galactic nuclei, [e.g. 18]). These results are, however, a strong prove of the tight relation between the synchrotron emission from the jet and the inverse Compton γ -ray emission.

There is already more, and much stronger, previous evidence in favor of the “far site” scenario nevertheless. Indeed, [19] reported that the γ -ray flares in blazars often happen after the initial stages of a prominent millimeter flare, which they interpret as the γ -ray flare produced either at or downstream the radio core of the jet. More recent work based on densely time sampled data from the Large Area Telescope (LAT) onboard the *Fermi* Gamma-ray Space Telescope has confirmed the same result from the group [13]. Also, the GeV and TeV spectra of blazars provide, in some cases, strong support in favor of the “far site” scenario. As described by [e.g. 20–22], not all blazars show the absorption features modeled by [7] as being produced by absorption within the BLR. The non-existence of such broad-band γ -ray absorption features, together with the known large photon-photon opacity of the BLR in such blazars, forces the γ -ray emission to be inverse Compton up-scattered from a jet region considerably away from the BLR.

Moreover, during the latest five years, the combination of ultra-high resolution very long baseline interferometric

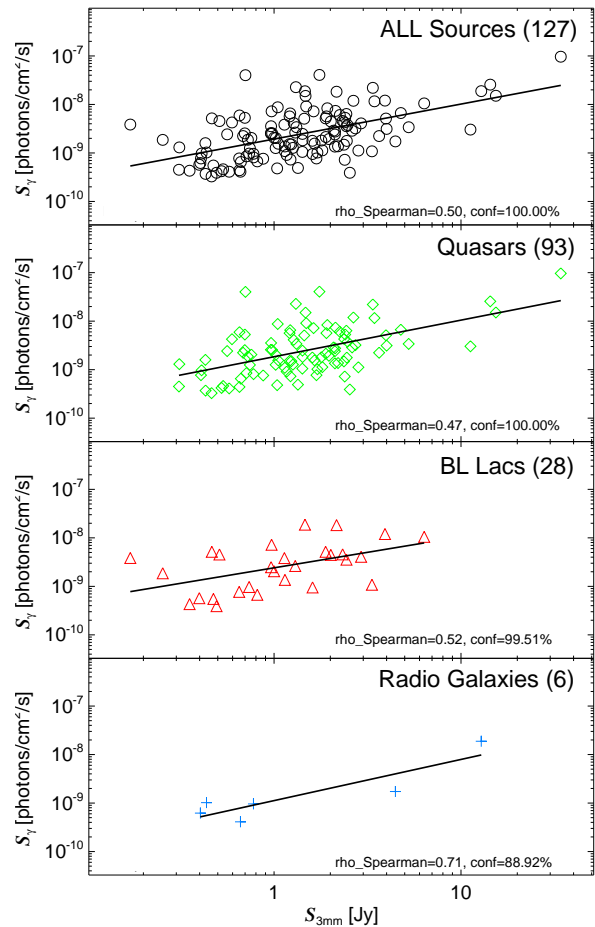


Figure 1. γ -ray flux versus 86 GHz (3.5 mm) total flux for all sources contained in the polarimetric-millimeter active-galactic-nuclei survey by [17], and in the 2LAC *Fermi*-LAT catalog. The sample of sources surveyed by [17] contains 211 bright millimeter blazars, and was designed to be flux limited at 1 Jy at 86 GHz. All data sets, except the less populated radio galaxy set, show statistically significant correlation above 99.7% confidence. The same result is obtained for the parallel 229 GHz (1.3 mm) measurements made for the above mentioned data set, see [17].

observations with the unprecedentedly well time sampled γ -ray light curves from the *Fermi*-LAT is providing further strength to the arguments in support for the “far site” scenario. The following sections in this paper describe the power of very long baseline interferometry (VLBI) observations for such kind of studies, as well as some additional recent results regarding the location of the γ -ray emission region in the “far site” of blazar jets.

4 VLBI and the Location of the γ -Ray Emission Site in Blazars

VLBI is the only astronomical technique so far able to resolve extragalactic jet structures at millimeter wavelengths in the sub-parsec scales up to high cosmological redshifts. Indeed, VLBI at 7 mm wavelengths provides angular res-

olutions of up to ~ 0.1 milliarcseconds (mas), which is several hundred times better than what the Hubble Space Telescope can do. Therefore, combining VLBI imaging programs to monitor blazars with densely-time-sampled γ -ray measurements, and light curves at other spectral ranges is a powerful tool to find the location of the γ -ray emission.

4.1 Some Historical Perspective

In a pioneering study using this method at the times of EGRET, onboard the Compton Gamma Ray Observatory, [23] monitored 42 γ -ray bright blazars with the Very Long baseline Array (VLBA) at 22 and 43 GHz from 1993 to 1997 to determine the jet proper motions and ejections that could be related to the γ -ray behavior observed by EGRET. This program showed that the apparent superluminal motions in γ -ray sources were much faster than for the general population of bright compact radio sources. An apparent correlation between the VLBI core flux density and the γ -ray flux of the monitored blazars was also reported. Both these results have been confirmed by recent work with *Fermi*-LAT data [e.g. 9, 10, 12].

On a second paper, [24] suggested that the γ -ray flaring events occur in the superluminal radio knots, and they derived a general pattern of behavior of the sources that is still valid for some events recently monitored with much better sensitivity, and time and spectral coverage. This is, a perturbation causes the ejection of a superluminal component close to the time where the linear polarization flux density reaches its minimum. This event is followed by a γ -ray flare, that happens almost at the same time of a radio linear polarization maximum. During the γ -ray flare, the polarization degree almost significantly increases with regard to the quiescent level and later comes back to the initial quiescent state. The “far site” scenario was not widely accepted within the blazar community at the time when this work was published, although it provided one of the first evidence suggesting that the γ -ray and the millimeter core of emission in the blazar jet might be co-spatial.

This early work provided the seed for a strong argument in favor of the “far site” scenario. There are reasons to consider that jets in blazars are not efficient synchrotron radio-millimeter emitters up to distances ≥ 0.1 pc from the central engine. After formation, the jet plasma needs some distance to get sufficiently energized to emit efficiently at millimeter wavelengths [see also 18, 25–28]. Therefore, if γ -ray emission and millimeter cores are co-spatial in blazars, they must be located at the position of the jet millimeter cores, that are considered to be placed relatively far from the central engine (see below).

4.2 More Recent Work

The advent of *Fermi*-LAT has implied a revolution in sensitivity by more than an order of magnitude with regard to EGRET. Together with this, the large field of view and the standard whole-sky survey mode of *Fermi*—which observes the entire sky several times per day since mid 2008—has allowed to obtain for the first time great detail γ -ray

light curves of bright blazars. The analysis of the γ -ray properties of *Fermi*-LAT source catalogs with those of different VLBI radio wavelength surveys have confirmed previous ideas derived from EGRET about the connection of the γ -ray and radio-mm emission in blazars [e.g. 9, 10, 12, 29].

Since around 2007, before the start of operations of the *Fermi* Gamma-ray Space Telescope, several international consortia have devoted large efforts to support comprehensive multi-spectral-range programs, including γ and X-rays with the NASA *Fermi* and *Swift* Space Observatories, to monitor bright γ -ray blazars. Current state-of-the-art observing programs include close monitoring of the flux from radio to γ -ray frequencies, monitoring of the polarization at radio to optical wavelengths, and direct imaging down to sub-milliarcsecond resolution at radio wavelengths with VLBI observations. Through correlation studies, such a kind of program allows the establishment of connections—and therefore relative locations—of the emission at different wavebands, and of associations of the variable emission with bright knots—imaged with VLBI—that move down the jet, usually at superluminal apparent speeds. Furthermore, polarization observations reveal the degree of ordering and mean direction of the magnetic field.

A good example of the success of this method was presented by [25] through a comprehensive multi-spectral range study of the jet in blazar PKS 1510–089 including densely time sampled light curves and monthly polarimetric 7 mm VLBA images of the jet in the source. This work reported the time coincidence of a prominent jet ejection with a bright γ -ray flare, an optical flare, a radio flare, a sharp optical polarization peak, and the end of an optical polarization swing by $\sim 700^\circ$. The time coincidence of all these events was the main argument to argue in favor of their inter-relation and co-spatiality with the actual position of the imaged bright moving knot detected on the VLBI images, that was located a ~ 20 pc from the central engine and beyond. Additional examples of this kind of studies, reaching similar conclusions through VLBI and multi-spectral range monitoring programs of blazars can be found in Marscher (these proceedings) and Jorstad et al. (these proceedings, see also [26]).

In the following sections the results from two additional studies on the bright blazars OJ287 and AO 0235+164 are presented in some detail. There two studies illustrate the power of using sequences of polarimetric millimeter VLBI images, that in combination with multi-spectral-range light curves, allow to reach unambiguous conclusions about the location of the flaring γ -ray emission in blazars, and about the mechanism for such γ -ray emission.

5 “Far Site” Location of the γ -ray flaring emission in AO 0235+164

AO 0235+164 is an extremely variable BL Lac object at all spectral ranges from radio wavelengths to γ -rays. This source underwent a drastic multi-spectral-range outburst

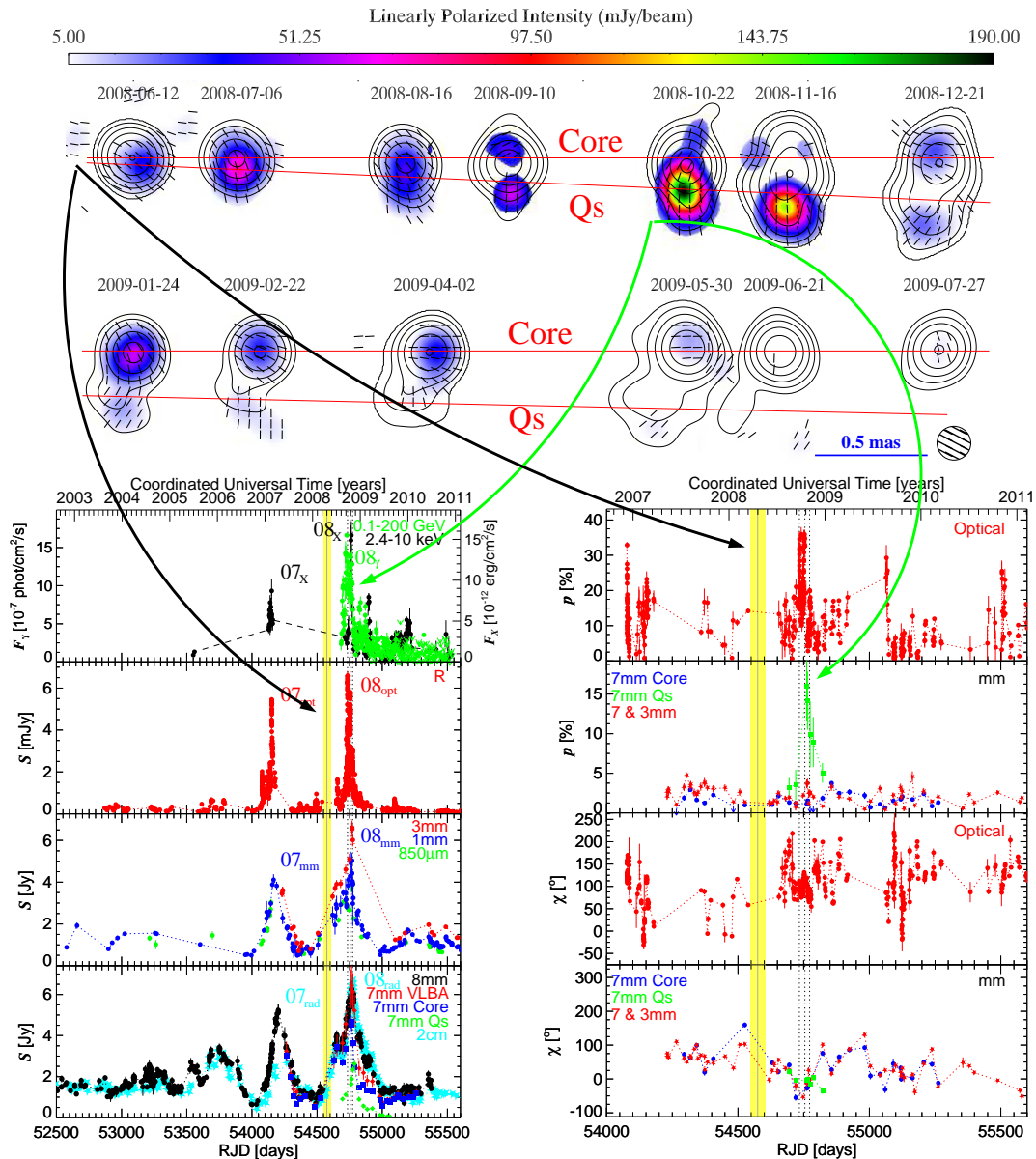


Figure 2. *Top:* Sequence of 7 mm VLBA images of AO 0235+164. All images were convolved with a common circular-Gaussian beam with FWHM = 0.15 mas. Contours symbolize total intensity observed (9 levels from 0.4 to 90.0 % of total intensity peak at = 4.93 mJy/beam), the color scale represents polarized intensity, whereas the distribution of short sticks show the orientation of the linear polarization angle χ . *Bottom-left:* Light curves of from γ -ray to radio. The vertical dotted lines represent the time of the three major optical peaks in the second half of 2008. The yellow area shows the ejection time range of feature Qs, including its uncertainty. *Bottom-right:* Optical and millimeter linear polarization curves of AO 0235+164.

peaking at the end of 2008. This extraordinary event was detected by *Fermi* at γ -rays, and was reproduced at essentially all remaining available spectral ranges down to radio wavelengths. In this section we describe the observing effort that we made to study the event, as well as our interpretation of the data. Most of the results presented here are reproduced from a paper published in [28].

On the sub-milliarsecond scales, AO 0235+164 shows a very compact structure (with an apparent extension $\lesssim 0.5$ mas) at millimeter wavelengths [e.g. 30], and displays superluminal apparent speeds [$\beta_{\text{app}}^{\text{max}} = 46.5 \pm 8.0 c$,

23]¹. This velocity, and the variability Doppler factor $\delta_{\text{var}} = 24.0$ of AO 0235+164 computed by [31], limits the jet viewing angle to a maximum $\theta = \arctan[2\beta_{\text{app}}^{\text{max}} / (\beta_{\text{app}}^{\text{max}2} + \delta_{\text{var}}^2 - 1)] \lesssim 2.4$. Several superluminal features were detected at position angles ranging from 5° to -55° [23, 30], which is consistent with a broad ($\alpha_{\text{app}} \approx 60^\circ$) jet opening-angle as projected in the plane of the sky. θ and α_{app} also

¹Throughout this paper we adopt the standard Λ CDM cosmology, with $H_0 = 71 \text{ km s}^{-1} \text{ Mpc}^{-1}$, $\Omega_M = 0.27$, and $\Omega_\Lambda = 0.73$. Hence, for AO 0235+164 ($z = 0.94$), 1 mas corresponds to a projected linear distance of 7.9 pc and a proper motion of 1 mas/yr implies a superluminal speed of $50 c$

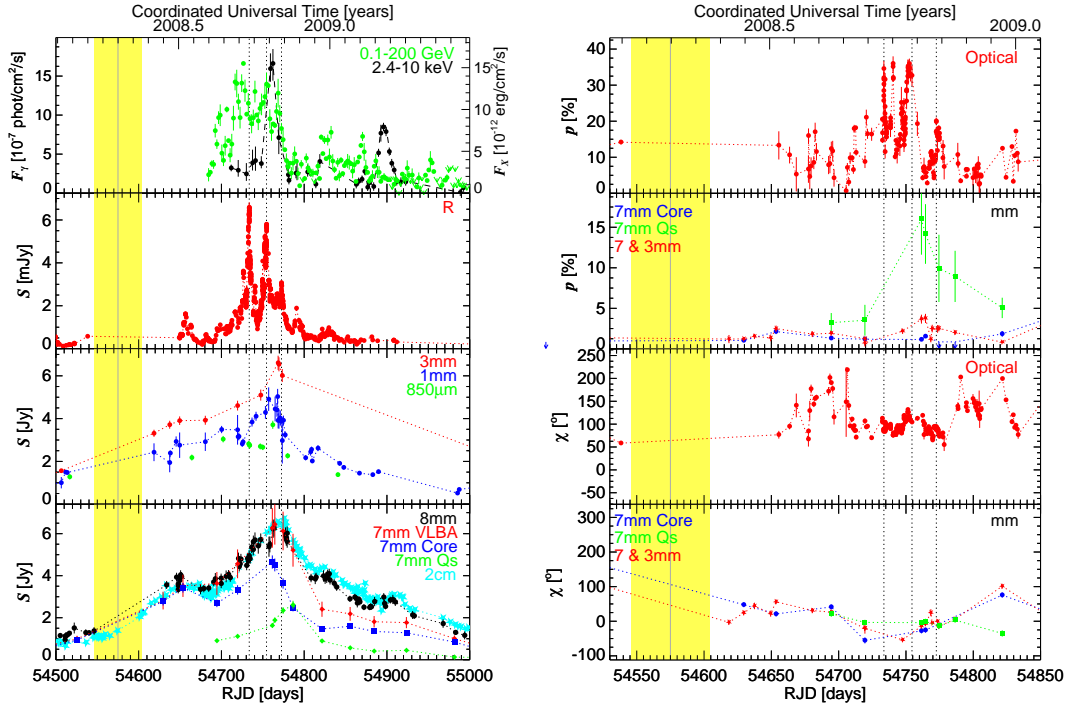


Figure 3. *Left:* Same as Fig. 2-bottom-left light curves of AO 0235+164, but zoomed into RJD=[54500,55000]. *Right:* Same as Fig. 2-bottom-right polarization evolution curves of AO 0235+164 but zoomed into RJD=[54530,54850].

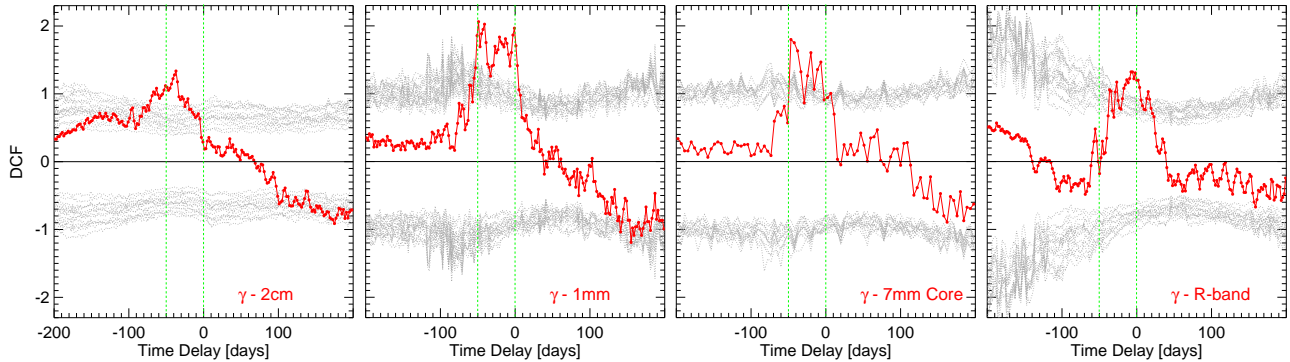


Figure 4. Grid of discrete correlation functions the γ -ray light curves in Fig. 2 and those at 2 cm, 1 mm, 7 mm (core), and optical (R-band) for AO 0235+164. The grey dotted curves at positive (negative) DCF values symbolize 99.7% confidence limits for correlation against the null hypothesis of stochastic variability. See [28] for details about the Monte-Carlo simulations performed to make this analysis.

limits the intrinsic jet half-opening-angle to be $\alpha_{\text{int}}/2 = (\alpha_{\text{app}} \sin \theta)/2 \lesssim 1:25$.

The photo-polarimetric monitoring data-set that we compiled from AO 0235+164 (Fig. 2) consisted on a set of 32 VLBA images at 7 mm images from the Boston University monthly blazar-monitoring program, 3.5 mm measurements with the IRAM 30 m Telescope, and optical observations from telescopes on several observatories. These optical telescopes include the 2.2 m Telescope at Calar Alto Observatory, the 2.3 and 1.54 m Telescopes at Steward observatory, the 1.83 m Perkins Telescope at Lowell, the 0.84 m Telescope at San Pedro Mártir, the 0.7 m Telescope at Crimean Astrophysical Observatory, and the 0.4 m Telescope at St. Petersburg State University. The

total flux light-curves shown in Fig. 2 also contain measurements from *Fermi*-LAT at γ -rays (0.1-200 GeV) and both *Swift* and *RXTE* at X-rays (2.4-10 keV). Other lower energy facilities from where we got measurements include the Tuorla Blazar Monitoring Program, the Yale University SMARTS program and Maria Mitchell Observatory in the optical R-band, the Submillimeter Array at 1.3 mm and 850 μm , the IRAM 30 m Telescope at 1.3 mm, the Metsähovi 14 m Telescope at 8 mm, and the Owens Valley Radio Observatory and University of Michigan Radio Astronomy Observatory 26 m Telescope at 2 cm. The data reduction procedures to calibrate the data were described in [28] (see also [25, 26, 32, 33]).

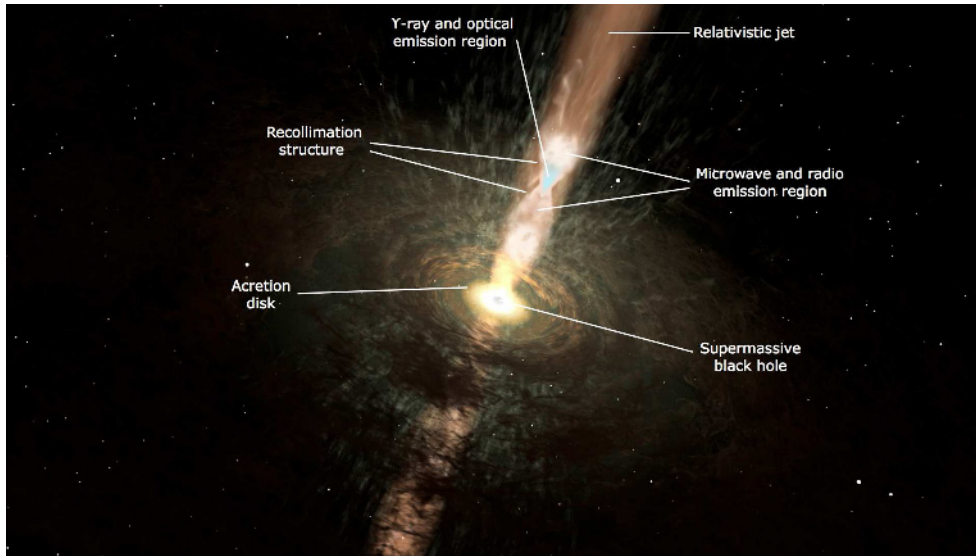


Figure 5. Conceptual representation of the physical interpretation of the multi-spectral-range correlated flaring activity reported for the case of AO 0235+164 (see the text). Image Credit, Wolfgang Steffen (UNAM).

5.1 Relation Between a Strong Superluminal Ejection in the Jet of AO 0235+164 and its Millimeter Flare in 2008

The VLBA 7 mm images of AO 0235+164 shown in Fig. 2 display a compact total intensity distribution that was fitted by a maximum of two circular Gaussian emission components for most observing epochs. The core of emission in our images (the feature systematically present in all observing epochs) was assumed to be the innermost millimeter emitting region in the jet. The jet structure, between mid-2008 and mid-2009, shows an additional emission region, i.e. Qs, which corresponds to the brightest 7 mm jet feature ever detected in AO 0235+164. Qs is also an extremely fast superluminal feature. Our model fits give an superluminal apparent speed $\langle \beta_{\text{app}} \rangle = (12.6 \pm 1.2) c$.

We estimate that the ejection of Qs happened in 2008.30 ± 0.08 , which coincides with the beginning of the extraordinary millimeter outburst (08_{mm} in Fig. 2) started in early 2008, and peaking (at $\sim 6.5 \text{ Jy}$ at 3 mm) on October 10th, 2008. In Fig. 2 we show that both the 08_{rad} and 08_{mm} radio and millimeter outbursts, that peak around October 20th and November 16th 2008; respectively, were produced by the contribution of both the VLBI core and Qs to the integrated emission from the source. The coherent -although delayed- behavior of the core and Qs suggests that the perturbation responsible for the ejection of Qs is extended from the position of the core to the one of Qs in the frame of the observer. This is consistent with the effect of light travel time delays for relativistic sources propagating towards the observer, that stretch the apparent size of the emission regions [e.g. 34, 35]. Furthermore, Qs is the only bright superluminal ejection happened during our monitoring program detected during the evolution of flares 08_{rad} and 08_{mm} . This allows us to unambiguously relate both the radio and mm flares with the ejection (and further evolution) of the Qs emission feature.

5.2 Correlated Flares from Radio Frequencies to γ -rays in AO 0235+164

Figure 2 reveals that the 08_{rad} and 08_{mm} flares happened at the same time as parallel optical, X-ray, and γ -ray outbursts (named 08_{opt} , 08_{x} , and 08_{γ} in Fig. 2, respectively). We made a formal correlation study of the light curves in Fig. 2 (see also [28]) which confirms the statistically significant correlation of the γ -ray flux evolution with the 2 cm, 1 mm, and optical light curves with a confidence $> 99.7\%$. Even the light curve obtained from the integrated emission within the 7 mm VLBI-core region is also correlated with the γ -ray light curve at $> 3\sigma$ confidence. The evolution of the optical polarization degree (p_{opt}) and the X-ray flux are also correlated with the optical R-band, 1 mm, and 2 cm light curves at high confidence (see [28]), hence indicating that the prominent flaring activity shown in Figs. 2 and 3 is related at all wavelengths from radio to γ -rays.

Note however that although there is clear correlation on the long time scales (of \sim years), there is not a common variability pattern at all spectral ranges on the short time scales ($\lesssim 2$ months). This reflects a different variability mode on the short and long time scales.

5.3 Total Flux Flares Accompanied by Extreme Linear Polarization Peaks in AO 0235+164

Figures 2 and 3 show extremely-high optical-polarization fraction ($p_{\text{opt}} \gtrsim 30\%$) and variability during the prominent optical flaring state 08_{opt} . The total millimeter polarization-degree (p_{mm}), and the polarization degree of the core are observed to lie at modest values of $\lesssim 5\%$. However, for Qs, $p_{\text{mm,Qs}}$ displays an extremely large peak at $\sim 16\%$ close to the time of the second sharp optical sub-flare, see Fig. 3. Such an extraordinary $p_{\text{mm,Qs}}$ peak -by far the brightest superluminal feature detected so far

in AO 0235+164- has not been observed in other previous VLBI jet features in the source. The coincidence of this prominent linear polarization peak of Qs with the bright optical flux and p_{opt} state, together with the flaring states at the other available spectral ranges (including the 7 mm-VLBI-core one), points out that the ejection (and propagation) of Qs is physically related to the multi-spectral-range flaring state at the end of 2008 and the extreme p_{opt} activity.

5.4 Interpretation of the AO 0235+164 Observations

The coincidence in time of the appearance and propagation of Qs in the jet of AO 0235+164 with the prominent γ -ray to radio flares in the end of 2008 and the exceedingly high p_{opt} and $p_{\text{mm,Qs}}$, evidences the physical relation of these events. This was confirmed by probabilistic arguments [28] -giving a probability $p_{\gamma,\text{opt,mm}} = 5 \times 10^{-4}$ that a γ -ray, an optical, and a radio to millimeter flare may occur contemporaneously by chance. Our formal correlation study based on the analysis of the discrete correlation function provides further support to this argument, see above and [28]. In [28], we located the 7 mm VLBI-core at a de-projected distance $\gtrsim 12$ pc from the vertex of the jet in AO 0235+164. This, together with the highly statistically significant correlation of the flare of the 7 mm core in 2008 with the multi-wavelength flares at the other available spectral ranges[28], suggest that the flares at these other spectral ranges were also located $\gtrsim 12$ pc from the central black hole in the central active galactic nuclei of AO 0235+164.

We assume that the 7 mm VLBI-core is a stationary recollimation structure at the end of the acceleration and collimation zone of the jet [18, 25] (see Fig. 5 for a sketch). If so, the fast superluminal component Qs should be related to a moving shock, given its extremely high $p_{\text{mm,Qs}}$. The fact that $\chi_{\text{mm}}^{\text{Qs}}$ is parallel to Qs's direction of propagation indicates that the shock front in Qs should be perpendicular to the jet axis. Moreover, the core and Qs show a rather similar flux evolution, which indicates the spatial extension of Qs. This suggests that Qs is the head of an extended structure stretched by light travel time-delays in the observer's frame, as e.g. the front-back structure reported by Ref. [36].

Multi-zone SSC scenarios, e.g. as those involving emission from different turbulence cells[37], are a likely possibility to explain the behavior of AO 0235+164 given its good multi-spectral-range correlation on the long time scales, but poorer short time-scale correlation. Figure 5 shows a sketch of the scenario that we proposed in [28] to explain the multi-spectral range behavior of the source. The radio, the millimeter, and the optical flares are proposed to be produced at the location of the 7 mm core (assumed to be a conical shock) by particle acceleration in a moving blob -Qs in the case of AO 0235+164- when it crosses the standing shock. After crossing the conical shock, the accelerated electrons in Qs also contribute to the flares, hence producing the long duration outbursts ob-

served in AO 0235+164. Shortly after this crossing, the γ -ray flares are proposed to be produced by inverse Compton scattering of the synchrotron optical-IR photons emitted from the core-Qs region.

Since we have identified the location of the multi-spectral-range flares to be at > 12 pc from the central engine, the BLR (typically at < 1 pc from the central black hole) cannot be a possible source for such seed optical-IR photons. Moreover, prominent IR emission from the dusty torus has not been detected so far in BL Lac objects such as AO 0235+164. This favors the synchrotron-self-Compton mechanism as the most probable cause of the flaring γ -ray emission in AO 0235+164. Further arguments, based on the properties of the long and short time scales of multi-spectral range variability, are given in [28] to support this hypothesis.

6 The ‘‘Far Site’’ γ -ray Emission in Flares of OJ287

Like in our previous study on AO 0235+164, we performed a similar study on the BL Lac object OJ287 ($z = 0.306$)². In particular, for OJ287 we also found a coherent relation in the multi-spectral range behavior of the source that underwent a series to two γ -ray flares at the end of 2008 and 2009 as detected by the *Fermi*-LAT. The polarimetric observations that we compiled for the study on OJ287 comprise 24 VLBA images at 7 mm, 3 mm observations with the IRAM 30 m Telescope, and optical observations from the 2.2 m Telescope at Calar Alto Observatory, the 2.3 and 1.54 m Telescopes at Steward observatory, the 1.83 m Perkins Telescope at Lowell, the 0.84 m Telescope at San Pedro Mártir, the 0.7 m Telescope at Crimean Astrophysical Observatory, and the 0.4 m Telescope at St. Petersburg State University, as well as the photo-polarimetric data compiled by [39] (Fig. 6). The total flux light curves come from the *Fermi*-LAT γ -ray (0.1–200 GeV) and *Swift* X-ray (0.3–10 keV) archives, and from the one by the Yale University SMARTS program. We also analyzed the data from the SMA at 1.3 mm and 850 μm , from the IRAM 30 m Telescope at 1.3 mm, and from the Metsähovi Radio Observatory 14 m Telescope at 8 mm (see Fig. 6). The reduction of our data followed the procedures given in [27], where an more extended explanation of the analysis and interpretation of the data can also be found.

6.1 Millimeter Flares Produced in an Emission Feature > 14 pc From the Core in OJ287

To facilitate the analysis of the VLBI data, we modeled the brightness distribution of the 7 mm images of OJ287 with a reduced number of circular Gaussian emission features. The most prominent ones are the core (the innermost emission feature jet upstream visible in our images, assumed to be stationary) and component a, see Fig. 6.

²At this redshift, 1 mas represents a distance of 4.48 pc in the plane of the sky, whereas a proper motion of 1 mas/yr corresponds to an apparent superluminal speed of 19 c .

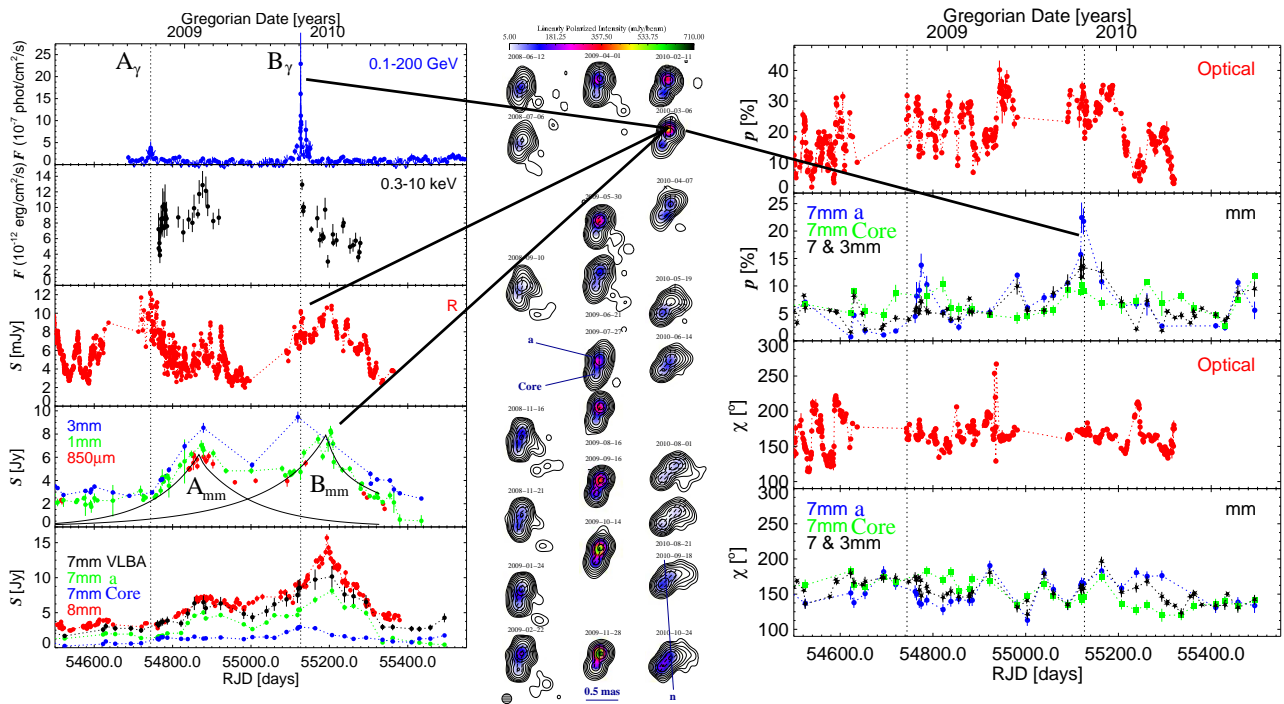


Figure 6. Left: Total flux light curves of OJ287 from γ -rays, to short millimeter wavebands. Middle: Sequence of 7 mm VLBA images compiled by [27]. All images were convolved with a common restoring circular-Gaussian-beam with FWHM = 0.15 mas. Contour levels start at 0.2 of the peak total intensity (6.32 Jy/beam) and increment by factors of two. The color scale represents linear polarization intensity, and black segments symbolize the distribution of position angles of the linear polarization. Right: Optical and millimeter wavelength linear-polarization-evolution curves of OJ287 compiled by [27].

The identification of the southern emission feature in our VLBA images as the innermost jet feature upstream is justified by the detection of a fast superluminal motion of feature n traveling from the core to a, and afterwards towards its west-southwest with an apparent speed of $\sim 10c$ (see [40] for further details and a complete argumentation).

Fig. 6 shows the most extreme 1 mm flares ever detected in OJ287 (A_{mm} and B_{mm}). These flares were produced in emission component a as shown by the correspondence of the 7 mm total flux evolution of component a and the ones at the remaining millimeter wavebands. Taking into account the certainty in the identification of the core in our images as the innermost jet emission feature detected in our images, and the de-projected distance between component a and the core (> 14 pc, as results from the half opening angle of jet –between $1^{\circ}9$ and $4^{\circ}1$ as reported by [1, 38]–, and the mean distance from the core and a [0.23 ± 0.01 mas]), we locate component a at > 14 pc from the central engine OJ287. Note that there should be an additional distance between the central black hole and the core (see above), and component a is already located at > 14 pc from the core.

6.2 Location of the γ -ray Flare Emission at the Millimeter VLBI Core in OJ287

As earlier reported for other sources by [19] and [13] through the combined analysis of light curves from EGRET and *Fermi*, respectively, and Metsähovi Radio

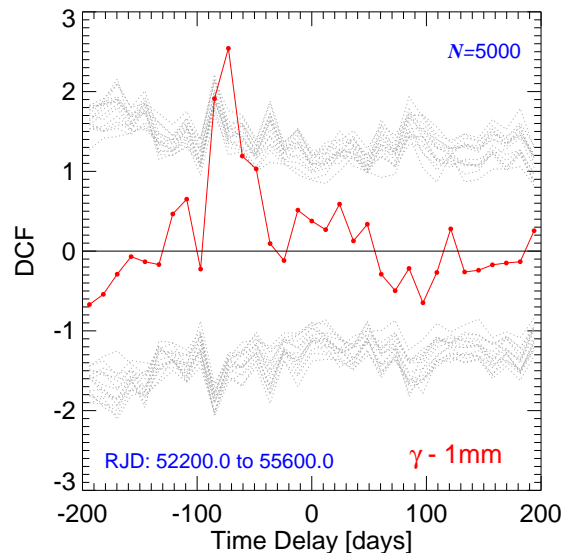


Figure 7. Discrete correlation function between the γ -ray and 1 mm light curves of OJ287 presented in [27]. The grey dotted curves denote the 99.7% confidence limits for correlation (and anti-correlation) against stochastic variability as derived from Monte-Carlo simulations, see [27] for details.

Observatory data, the prominent A_{mm} and B_{mm} flares in OJ287 start to rise at the time of two sharp γ -ray flares (see Fig. 6). These two γ -ray outbursts, that peaked on 2008 October 4 and 2009 October 24, show 0.1–200 GeV

photon fluxes that exceed the quiescent γ -ray level of the source by a factors ~ 2 and ~ 5 , respectively.

The discrete correlation function between the 1 mm and the γ -ray light curves (Fig. 7), shows a clear peak at a time lag ~ -80 days. Indeed, our Monte-Carlo simulations testing the statistical significance of the correlation prove that such peak is significant at 99.7% confidence against stochastic variability, which confirms the correlation between B_γ and B_{mm} . These are the two brighter γ -ray and 1 mm flares reported from our data. Finally, the good correspondence of the 7 mm light curve of VLBI component a and the 1 mm light curve of OJ287 sets the location of B_γ flare at the position of component a.

The optical light curve in Fig. 6 displays two prominent and sharp peaks at the time of A_γ and B_γ γ -ray flares. Nevertheless, the sparser time sampling of the X-ray light curve do not permit us to claim for a relation between the γ -ray and X-ray variability. This is a possibility that cannot be ruled out though.

6.3 Relation of Multi-Spectral-Range Flares and the Linear Polarization Variability in OJ287

Although the time evolution of the linear polarization angle (χ) of the core and component a is similar, these two emission features are rather different in which regards to the properties of their p variability (see Fig. 6). The core do not even reach linear polarization degree values $p \approx 10\%$, whereas component a shows the two largest peaks in 7 mm linear polarization (with $p \approx 14\%$ on $\sim 2008-11-04$, and $p \approx 22\%$ on $\sim 2009-10-16$) that have ever been reported in OJ287. These two extreme linear polarization peaks of component a happened contemporaneously with the A_γ and B_γ γ -ray flares. The peak in the linear polarization degree at millimeter wavelengths that occurred in the end of 2008 is delayed by ~ 15 days with regard to A_γ , but the second one ($p \gtrsim 22\%$) is consistent with being simultaneous with the extreme B_γ γ -ray peak. We consider the coincidence of these two latest exceptional events as a strong evidence in support of the idea that both happened co-spatially, being component a located at > 14 pc from the central engine (see above).

The linear polarization degree at optical wavelengths varies faster, and much strongly, than the one at short millimeter wavelengths. This is consistent with the frequency dependence predicted in the blazar internal turbulence model by [37]. Also, sharp linear polarization degree peaks in the optical occur at essentially the same time as the peaks of A_γ and B_γ γ -ray flares. Nonetheless, other similar optical polarization peaks happen also at other times not related to the γ -ray flares.

On the other hand, the polarization angle at optical and millimeter wavelengths is clearly stable at $\chi \approx 160^\circ-170^\circ$ —which is similar to the inner jet's position angle—either at the times of the γ -ray flares, and during the overall time evolution of OJ287 covered by our study. Such χ stability is only significantly altered in sporadic and short duration optical rotations of by up to 180° , see also [39], which is consistent with the turbulent blazar model by [37].

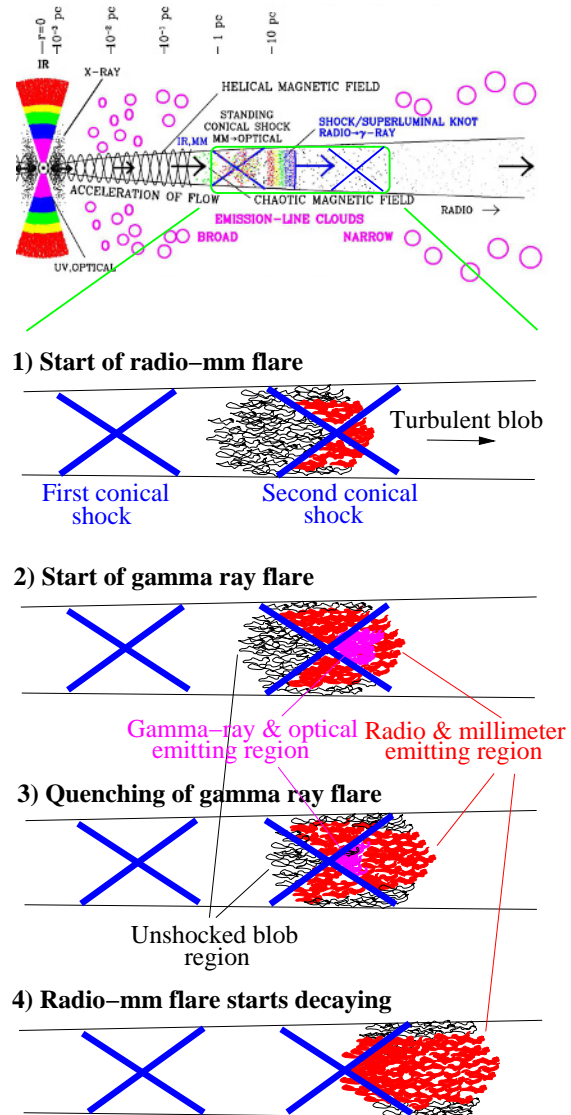


Figure 8. Conceptual illustration of the proposed scenario for the multi-spectral-range behavior of OJ287 reported in [27], see the text. Credit for quasar cartoon at the top of the figure: Alan P. Marscher (Boston University).

6.4 Interpretation of the Multi-Spectral-Range Observations of OJ287

The analysis of our multi-spectral-range observations of OJ287 allowed us to report about a number of coincidences in the total flux and and polarimetric behavior of the source. These comprise: *a*) two extreme γ -ray flares that peaked in October 2008 and 2009 (A_γ and B_γ , respectively), *b*) the rising phase of the two most luminous 1 mm flares so far reported in OJ287 (A_{mm} and B_{mm}), that our 7 mm VLBA image sequence locates unambiguously at the position of component a, *c*) two sharp optical flares, and *d*) two extreme linear polarization degree peaks at the location of component a. The latter polarization peaks did not correspond to any significant linear polarization angle variability. Rather, χ clustered around a mean value $\bar{\chi}_{\text{mm}} \approx 160^\circ-170^\circ$. Moreover, the large linear polariza-

tion degree of component a during the second γ -ray flare further supports the location of the γ -ray events at the position of component a.

The γ -ray inverse Compton emission detected by *Fermi* may have been produced from either the synchrotron self-Compton mechanism or by inverse Compton scattering of IR radiation from the dusty torus. However, IR emission from the dusty torus has not been detected so far in BL Lacs like OJ287. Also, the BLR photon field is not a possible seed for the up-scattering up to γ -rays for the OJ287 flares that we have reported. First, OJ287 is a BL Lac object with very weak or inexistent BLR emission. Second, the far location of the γ -ray emission region in the source that we report completely rules out the BLR photon field because of its short distance to the central engine. In contrast, a synchrotron self-Compton model is possible given the relatively small γ -ray to synchrotron luminosity ratio; ≈ 2 in OJ287, see [27].

Therefore, in [27], we proposed a scenario in which optical and γ -ray flares are produced by particle acceleration in component a (that we interpret as a conical standing shock following e.g. [34, 35]), when a traveling jet perturbation interacts with such component a at > 14 pc from the core and the central engine in OJ287, see Fig. 8. The traveling jet perturbation must be a turbulent plasma blob with higher relativistic electron density and magnetic field than in the jet flow. The turbulence in this feature is needed to explain the weak millimeter polarization observed far from the polarization peaks. This scenario was studied by [41], whose model reproduces the polarization properties observed in OJ287. This is, high polarization degree peaks happening at the time of the interaction of turbulent blobs with a conical shock, and χ parallel to the jet axis (see also [27]).

In our scenario, the optical and millimeter outburst begin with the increase of the magnetic field intensity and electron energy density of the traveling perturbation when it interacts with the stationary conical shock at the location of the core. The millimeter flares continue on as far as the low-energy electrons cross the conical shock. The optical and γ -ray flares, that are produced by higher-energy electrons, are dumped near the conical shock because of the faster cooling times of such electrons. Note that if synchrotron losses were the sole mechanism producing the optical emission dumping in flares, then the optical and γ -ray emission would be constant after the shocked jet feature fills the entire layer after the shock (at least before the entire jet feature crosses the conical shock). However, if the synchrotron-self-Compton mechanism dominates, the radiative losses are enhanced until the γ -ray losses start to be efficient, when electrons emitting optical synchrotron lose most of their energy and hence the optical flare is dumped. Because of this reason, we further support the synchrotron-self-Compton mechanism as the responsible one of the γ -ray emission in flares in OJ287.

7 General Considerations

It is notable that the detailed studies of the VLBI and multi-spectral-range variability properties of the jets in

OJ287 as in AO 0235+164 have allowed us to reach rather similar general conclusions, although there are indeed remarkable differences on the properties and behavior of these two sources. On the previous sections, it has been pointed out that, in contrast to other models that assume the γ -ray flaring emission of blazars to come from jet regions at distances $\ll 1$ pc from the central active galactic nuclei, the γ -ray flares have been located at > 12 pc from the central super-massive black hole for the case of the jets in the BL Lac objects AO 0235+164 and OJ287. It is important to remark that this result, for the case of both sources, is independent of any kind modeling, because it comes directly from the analysis of the observational data. Therefore, it represents a robust evidence in favor of the “far site” scenario for γ -ray emission in blazars.

This does not mean that this scenario can be generalized for the entire blazar class though. Indeed, there are several other sources with a completely different multi-spectral-range behavior that do not allow for the lines of argumentation presented above for AO 0235+164 and OJ287. Moreover, there are even other sources for which the bulk of the γ -ray emission is most likely produced in different jet regions or by different emission mechanisms. Perhaps adding some complication to the problem, it does not seem unnatural to think in particular sources where there is not a clear dominance of a single γ -ray production mechanism. In this later case, the high energy emission would need to be understood as a combination of more than one emission process.

We are still not close from drawing a general paradigm for the location of the γ -ray emission site and its responsible emission mechanism. Although we have already obtained some important insights into these problems, blazars display too wide a range of characteristics for us to claim that we understand their jets well. The complexity of γ -ray flares with different properties -e.g., some accompanied by optical polarization angle rotations and others not, or some with optical total flux flares and others not- indicates that there are multiple scenarios on which a general paradigm for the innermost regions of blazar jets can be based. Continued monitoring will allow for observing as much, and as robust relations as possible between the high-energy emission region of jets in active galactic nuclei and the inner jet regions resolved in ongoing ultra-high resolution VLBI monitoring projects. Only then a general paradigm for the location of the γ -ray emission site and its responsible emission mechanism can be drawn. For that, studies employing the ultra-high-resolution and polarimetric imaging capabilities of millimeter VLBI monitoring programs with time samplings sufficiently short for every particular source will be essential. Only using such kind of programs the absolute position of the millimeter emission features –in some cases responsible for the flaring emission at the remaining spectral ranges– can be directly imaged.

8 Acknowledgements

The author acknowledges the stimulating collaboration of Alan P. Marscher and Svetlana G. Jorstad, which was

more than essential for achieving the scientific results outlined in this, and in other work. The research presented in this manuscript was partly funded by NASA grants NNX08AJ64G, NNX08AU02G, NNX08AV61G, and NNX08AV65G, NSF grant AST-0907893, NRAO award GSSP07-0009; RFBR grant 09-02-00092; MICIIN grant AYA2010-14844; CEIC grant P09-FQM-4784; and GNSF grant ST08/4-404. The VLBA is an instrument of the NRAO, a facility of the NSF operated under cooperative agreement by AUI. The PRISM camera at Lowell Observatory was developed by Janes et al. The Calar Alto Observatory is jointly operated by MPIA and IAA-CSIC. The IRAM 30 m Telescope is supported by INSU/CNRS, MPG, and IGN. The SMA is a joint project between the SAO and the Academia Sinica.

References

- [1] Jorstad, S. G., et al., *AJ*, **130**, 1418 (2005)
- [2] Blandford, R. D. & Payne, D. G., *MNRAS*, **199**, 883 (1982)
- [3] Ackermann, M. et al., *ApJ*, **721**, 1383 (2010)
- [4] Foschini, L., et al., *MNRAS*, **408**, 448 (2010)
- [5] Foschini, L., et al. 2011, *A&A*, **530**, A77 (2011)
- [6] Tavecchio, F., et al., *MNRAS*, **405**, L94 (2010)
- [7] Poutanen, J. & Stern B., *ApJ*, **717**, L118 (2010)
- [8] Finke, J. & Dermer, D., *ApJ*, **714**, L303 (2010)
- [9] Kovalev, Y. Y., et al., *ApJ*, **696**, L17 (2009)
- [10] Lister M. L., et al., *ApJ*, **696**, L22 (2009)
- [11] Mahony, E. K., et al., *ApJ*, **718**, 587 (2010)
- [12] Pushkarev, A. B., et al., *ApJ*, **722**, L7 (2010)
- [13] León-Tavares, J., et al., *A&A*, **532**, A146 (2011)
- [14] Ackermann, M., et al., *ApJ*, **741**, 30 (2011)
- [15] Ghirlanda, G. et al., *MNRAS*, **407**, 791 (2010)
- [16] Ghirlanda, G. et al., *MNRAS*, **413**, 852 (2011)
- [17] Agudo, I., et al., *A&A* (submitted)
- [18] Marscher, A. P., et al., *Nature*, **452**, 966 (2008)
- [19] Lähteenmäki, A., & Valtaoja, E., *ApJ*, **590**, 95 (2003)
- [20] Sikora, M., et al., *ApJ*, **704**, 38 (2009)
- [21] Tavecchio, F., et al., *A&A*, **534**, A86 (2011)
- [22] Tavecchio, F., et al., *MNRAS*, **435**, L24 (2013)
- [23] Jorstad, S. G., et al., *ApJS*, **134**, 181 (2001a)
- [24] Jorstad, S. G., et al., *ApJ*, **556**, 738 (2001b)
- [25] Marscher, A. P., et al., *ApJ*, **710**, L126 (2010)
- [26] Jorstad, S. G., et al., *ApJ*, **715**, 362 (2010)
- [27] Agudo, I., et al., *ApJ*, **726**, L13 (2011a)
- [28] Agudo, I., et al., *ApJ*, **735**, L10 (2011b)
- [29] Lister, M. L., et al., *ApJ*, **742**, 27 (2011)
- [30] Piner, B. G., et al., *ApJ*, **640**, 196 (2006)
- [31] Hovatta, T., et al., *A&A*, **494**, 527 (2009)
- [32] Agudo, I., et al., *A&A*, **456**, 117 (2006)
- [33] Agudo, I., et al., *ApJS*, **189**, 1 (2010)
- [34] Gómez, J. L., et al., *ApJ*, **482**, L33 (2010)
- [35] Agudo, I., et al., *ApJ*, **549**, L183 (2001)
- [36] Aloy, M.-Á., et al., *ApJ*, **585**, L109 (2003)
- [37] Marscher, A. P. & Jorstad, S. G., in *Fermi Meets Jansky-AGN at Radio and Gamma-rays*, ed. T. Savolainen et al., 171 (2010)
- [38] Pushkarev, A. B., et al., *A&A*, **507**, L33 (2009)
- [39] Villforth, C., et al., *MNRAS*, **402**, 2087 (2010)
- [40] Agudo, I., et al., *ApJ*, **747**, 63 (2012)
- [41] Cawthorne, T. V., *MNRAS*, **367**, 851 (2006)